Phenomenology of Zn diffusion and incorporation in InP grown by organometallic vapor-phase epitaxy (OMVPE)

E. F. Schubert,[a] C. J. Pinzone, and M. Geva
AT&T Bell Laboratories, Murray Hill, New Jersey 07974

(Received 13 March 1995; accepted for publication 18 May 1995)

The diffusion characteristics and incorporation characteristics of Zn dopants in OMVPE-grown InP are studied. The Zn diffusion constant depends strongly on concentration and increases by four orders of magnitude in the Zn concentration range $2\times10^{18}-8\times10^{18}$ cm^{-3}. This drastic concentration dependence of the Zn diffusion constant is shown to determine the Zn incorporation characteristics during OMVPE growth. A spread of Zn dopants into intentionally undoped regions may result at high Zn doping concentrations in InP. © *1995 American Institute of Physics.*

Zinc (Zn) is the most frequently used acceptor in InP based compounds grown by organometallic vapor-phase epitaxy (OMVPE).[1] The characteristics of Zn dopants are (i) high electrical activity, (ii) moderate diffusion at concentrations $<10^{18}$ cm^{-3}, (iii) controllable incorporation with no "memory" effect, and (iv) low residual toxicity.[2–7] These characteristics make Zn preferable in InP over other *p*-type dopants such as Be, Cd, and Mg. High doping concentrations are desirable in many semiconductor devices in order to reduce parasitic resistances and *RC* time constants. However, it has been shown that the incorporation of Zn at doping levels in the 10^{18} cm^{-3} regime is problematic[8,9] and that Zn doping levels in the high 10^{18} cm^{-3} range cannot be achieved by epitaxial growth.

It is the purpose of this study to investigate the diffusion characteristics of Zn in InP. We show that the diffusion characteristics display a strong dependence on concentration. We further show that the diffusion characteristics are instrumental in the incorporation process of Zn during OMVPE.

The InP layers were grown by OMVPE on ⟨001⟩ oriented InP substrates. The horizontal flow growth system uses trimethylgallium, trimethylindium, diethylzinc, arsine, and phosphine as precursors. The epitaxial layers consist of a first 0.5 μm thick undoped InP buffer layer, a uniformly Zn doped layer with thicknesses of either 200 Å and 2000 Å, a second 0.5 μm thick undoped InP layer, and a 0.2 μm thick GaInAs cap layer. The ternary GaInAs cap was included to reduce the sensitivity of Zn diffusion on the ambient during annealing. Subsequent to the epitaxial growth, the samples were annealed (i) in the growth chamber under phosphine overpressure and (ii) in an AG Associate 410 rapid thermal annealer with the epitaxial side of the wafers covered by another InP wafer in order to reduce the outdiffusion of group-V elements. The Zn doping profiles were measured by secondary ion mass spectrometry (SIMS) using 5.5 keV primary Cs^+ ions and a sputter rate of 80 Å/s. Relative sensitivity factors were derived from InP:Zn implant standards.

The SIMS profiles of Zn dopants in InP for an as-grown sample and a sample annealed at 700 °C for 200 s are shown in Figs. 1(a) and 1(b), respectively. The intended width of the Zn doping pulse is 200 Å. Upon annealing, the SIMS profile width increases from 253 to 369 Å. The broadening of the profile is accompanied by a decrease in peak concentration from 4×10^{17} cm^{-3} to 2×10^{17} cm^{-3}.

The changes in peak concentration and profile width allow us to deduce the diffusion constant of Zn in InP. In the following analysis, we assume that the diffusion constant of Zn is, *within a small concentration range,* independent of the Zn concentration. This allows us to model the Zn dopant profiles in terms of Gaussian distributions. Assuming that the Zn peak concentration before and after annealing is N_1 and N_2, respectively, the diffusion constant D is given by

$$\sqrt{2Dt}=\sigma_1(N_1^2/N_2^2-1)^{1/2}, \tag{1}$$

where t is the annealing time and σ_1 is the standard deviation of the initial Gaussian distribution. The full-width at half-maximum (FWHM) of the initial dopant distribution and σ_1 are related by $\mathrm{FWHM}_1=2\sqrt{2\ \ln n\ 2}\sigma_1$. Using Eq. (1), a diffusion constant of 1×10^{-14} cm^2/s is deduced from the experimental data shown in Fig. 1.

The diffusion constant can be also inferred from the change in profile width using

$$\sqrt{2Dt}=(\sigma_2^2-\sigma_1^2)^{1/2}, \tag{2}$$

where σ_2 is the standard deviation of the profile width after thermal annealing. The standard deviation can be inferred from $\mathrm{FWHM}_2=2\sqrt{2\ \ln 2}\sigma_2$. We have also modeled the Zn profiles using a concentration dependent diffusion constant.

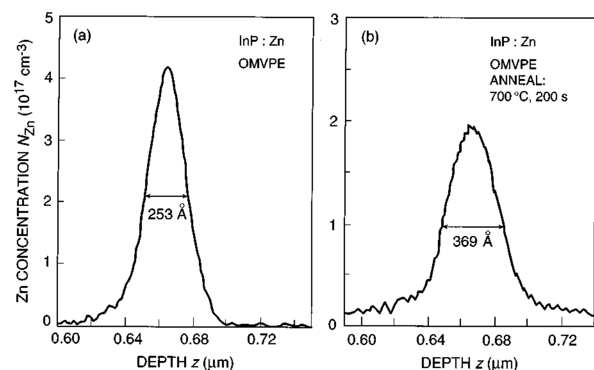

FIG. 1. Secondary ion mass spectrometry profile of a Zn doping spike in InP grown by OMVPE (a) before annealing and (b) after annealing under *P* overpressure at 700 °C for 200 s.

[a]Electronic mail: efs@clockwise.att.com

 0003-6951/95/67(5)/700/3/$6.00 © 1995 American Institute of Physics

Downloaded¬27¬Jun¬2003¬to¬128.113.111.105.¬Redistribution¬subject¬to¬AIP¬license¬or¬copyright,¬see¬http://ojps.aip.org/aplo/aplcr.jsp

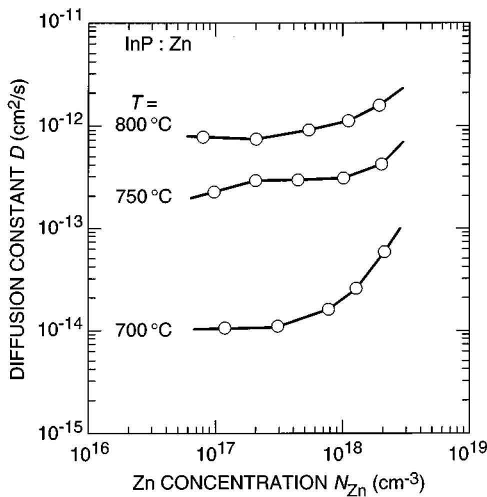

FIG. 2. Diffusion constant of Zn in InP as a function of Zn concentration for the three temperatures 700, 750, and 800 °C.

Comparison of these models with experimental profiles yields similar diffusion constants as compared to the results obtained from Eqs. (1) and (2).

The diffusion constants of Zn in InP are shown in Fig. 2 as a function of the Zn concentration. The diffusion constant displays a general trend of an increasing diffusion constant with Zn concentration. At Zn concentrations $< 10^{18}\ \mathrm{cm}^{-3}$, this trend is sublinear, i.e., weaker than a $D \propto N_{\mathrm{Zn}}$ dependence.

It is well known, that Zn doping concentrations exceeding $3\times10^{18}\ \mathrm{cm}^{-3}$ cannot be achieved during epitaxial growth by OMVPE or any other epitaxial growth technique.[1,8,9] In order to determine the diffusion constant of Zn in InP at concentrations exceeding $3\times10^{18}\ \mathrm{cm}^{-3}$, Zn must be diffused into InP from an external source.[10,11] Combining this experimental technique with the one outlined above yields the Zn diffusion constant in the entire concentration range of interest.

Figure 3 shows the diffusion constant of Zn in InP over a large concentration range for a diffusion temperature of

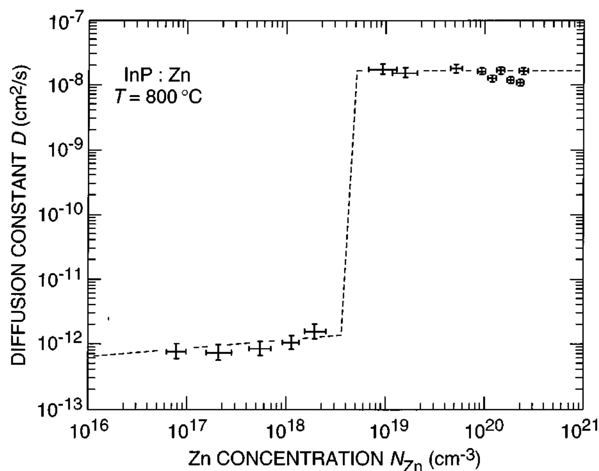

FIG. 3. Diffusion constant of Zn in InP at 800 °C as a function of Zn concentration.

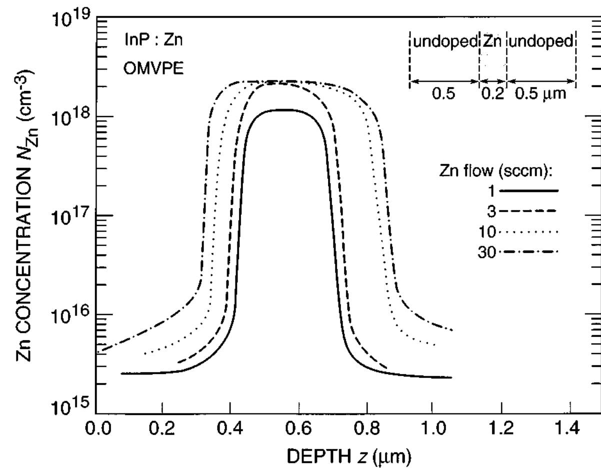

FIG. 4. Secondary ion mass spectrometry profile of Zn-doped InP grown by OMVPE at different Zn precursor flows given in sccm.

$T=800$ °C. At Zn concentrations $\leqslant 2\times10^{18}\ \mathrm{cm}^{-3}$, the diffusion constant is approximately $10^{-12}\ \mathrm{cm}^2/\mathrm{s}$. For Zn concentrations $\geqslant 8\times10^{18}\ \mathrm{cm}^{-3}$, the diffusion constant is approximately $10^{-8}\ \mathrm{cm}^2/\mathrm{s}$.[11] The striking feature displayed in Fig. 3 is the drastic increase of the diffusion constant in the narrow concentration range $2\times10^{18}\ \mathrm{cm}^{-3} \leqslant N_{\mathrm{Zn}} \leqslant 8\times10^{18}\ \mathrm{cm}^{-3}$. The magnitude of this increase comprises four orders of magnitude. We point out that at the present time, no suitable model explaining the drastic change in diffusion constant exists. Conventional models,[12] including defect-assisted diffusion and the substitutional-interstitial model cannot account for the peculiar dependence of the diffusion constant displayed in Fig. 3.

The distinctive concentration-dependence of the diffusion constant influences the Zn incorporation during epitaxial growth. Figure 4 shows the Zn doping profiles of four different InP samples grown with four different diethylzinc precursor flows, i.e., 1, 3, 10, and 30 standard cm^3 per minute (sccm). The inset of Fig. 4 depicts the intended doping distribution. At the lowest Zn precursor flow (1 sccm), the measured Zn doping profile agrees with the intended profile. However, for higher Zn fluxes, the Zn concentration reaches a maximum of $2.2\times10^{18}\ \mathrm{cm}^{-3}$ which is not exceeded even at the highest Zn precursor flow. Instead, the Zn profile broadens significantly and Zn diffuses towards the substrate as well as towards the surface of the epitaxial layer. At a Zn flow of 30 sccm, the profile broadens from the intended profile width of 0.2 μm to a measured profile width of 0.45 μm.

The incorporation characteristics of Zn into InP can be understood on the basis of the strong concentration dependence of the Zn diffusion constant. As the intended doping level exceeds $2\times10^{18}\ \mathrm{cm}^{-3}$, Zn atoms diffuse very rapidly. As a result, Zn doping profiles broaden at high concentrations, beyond their intended distribution width.

We point out that the concentration of $2.2\times10^{18}\ \mathrm{cm}^{-3}$, which is the maximum achievable concentration during our OMVPE growth experiments, is not a solubility limit. Transmission electron microscopy did not reveal any evidence of Zn precipitates even at the highest Zn precursor flows. The absence of precipitations is consistent with a solubility limit

Downloaded¬27¬Jun¬2003¬to¬128.113.111.105.¬Redistribution¬subject¬to¬AIP¬license¬or¬copyright,¬see¬http://ojps.aip.org/aplo/aplcr.jsp

of 10^{20} cm^{-3} at a growth temperature of 635 °C, which has been determined by Chang and Pearson.[10] However, the concentration of 2.2×10^{18} cm^{-3} may be the highest concentration, at which Zn incorporates on substitutional sites. Yu *et al.*[4] found evidence of abundant Zn interstitials at Zn concentrations exceeding 5×10^{18} cm^{-3}. For Zn concentrations $<2.2\times10^{18}$ cm^{-3}, Zn interstitials cannot be a significant fraction of the overall Zn concentration, due to the very high electrical activity of Zn in InP.

In conclusion, we have studied the phenomenology of Zn diffusion and incorporation in InP during OMVPE growth. The diffusion constant of Zn in InP depends strongly on concentration in the mid 10^{18} cm^{-3} range and increases by four orders of magnitude in the concentration range 2×10^{18}–8×10^{18} cm^{-3}. During OMVPE growth, the Zn concentration in the InP epitaxial layer cannot exceed a level of 2×10^{18} cm^{-3} due to the onset of rapid Zn diffusion. At Zn concentrations exceeding this level, rapid diffusion broadens Zn doping profiles beyond the intended distribution width.

We acknowledge the contributions of S. N. G. Chu and R. A. Logan.

[1] G. B. Stringfellow, *Organometallic Vapor-Phase Epitaxy* (Academic, San Diego, 1989).
[2] S. Chichibu, M. Kushibe, K. Eguchi, M. Fenemizu, and Y. Ohba, J. Appl. Phys. **68**, 859 (1990).
[3] A. Molassioti, F. Scholz, and Y. Gao, J. Cryst. Growth **102**, 974 (1990).
[4] K. M. Yu, W. Walukiewicz, L. Y. Chan, R. Leon, E. E. Haller, J. M. Jaklevic, and C. M. Hanson, J. Appl. Phys. **74**, 86 (1993).
[5] A. W. Nelson and L. D. Westbrook, J. Appl. Phys. **55**, 3103 (1984).
[6] C. J. Pinzone, N. T. Ha, N. D. Gérrard, R. D. Dupuis, and H. S. Luftman, Mater. Res. Soc. Symp. Proc. **163**, 867 (1990).
[7] A. W. Nelson and L. D. Westbrook, J. Cryst. Growth **68**, 102 (1984).
[8] W. T. Tsang, F. S. Choa, and N. T. Ha, J. Electron. Mater. **20**, 541 (1991).
[9] F. G. Kellert, S. R. Sloan, M. J. Ludowise, and J. E. Turner, J. Electron. Mater. **21**, 983 (1992).
[10] L. L. Chang and G. L. Pearson, J. Appl. Phys. **35**, 374 (1964).
[11] Diffusion data for $N_{Zn}>8\times10^{18}$ cm^{-3} shown in Fig. 3 were first published by M. A. Kadhim and B. Tuck, J. Mater. Sci. **7**, 68 (1972).
[12] E. F. Schubert, *Doping in III–V Semiconductors* (Cambridge University Press, Cambridge, 1993), p. 291.

Downloaded¬27¬Jun¬2003¬to¬128.113.111.105.¬Redistribution¬subject¬to¬AIP¬license¬or¬copyright,¬see¬http://ojps.aip.org/aplo/aplcr.jsp